Biotechnology Reports 42 (2024) e00838

Contents lists available at ScienceDirect

Biotechnology Reports

journal homepage: www.elsevier.com/locate/btre

Research Article

Biosynthesis, characterization and study of the application of silver nanoparticle for 4-nitrophenol reduction, and antimicrobial activities

Mengistu Mulu [a,b,*], Molla Tefera [a], Atnafu Guadie [a], K. Basavaiah [b]

[a] Department of Chemistry, College of natural and computational sciences, University of Gondar, Ethiopia
[b] Department of Inorganic and analytical Chemistry, Andhra University, India

ARTICLE INFO

Keywords:
Silver nanoparticle
Vigna unguiculata (L) Walp plant
4-nitrophenol
Antibacterial activity

ABSTRACT

Silver nanoparticles (AgNPs) were synthesized from *Vigna unguiculata* (L) Walp extracted leaves, and characterized. The UV–Visible spectrum showed a peak between 411 and 415 nm at the Plasmon absorbance of the AgNPs. TEM showed that the size of AgNPs ranged from 5 to 13 nm. It was spherical with an average size of 11.08 nm. The size of AgNPs was 7 ± 6 nm and disperse in water. The AgNPs effectively reduced 4-Nitrophenol (4-NP) to 4-aminophenol (4-AP) in the presence of $NaBH_4$. The AgNPs exhibited a strong antioxidant and antibacterial activity against Gram-negative bacteria: *Escherichia coli* (E. coli) and Klebsiella pneumonia and Gram-positive: *Bacillus pumilus* and *Staphylococcus aureus*. The average zones of inhibition of AgNPs were: 29 mm for *Staphylococcus aureus*, 23 mm for *Bacillus pumilus*, 17 mm for Klebsiella pneumonia and 15 mm for *Escherichia coli* (E. coli). Thus, AgNPs has exhibted good antibacterial activity compared to antibiotics drug and 4-NP reduction.

1. Introduction

Currently, materials production at the nanoscale has captivated the interest of many researchers due to the development of new materials with unique properties [1,2]. Nanomaterials are widely employed in treating human health, industrial fields, pharmaceutical applications, electronics, engineering, biomedical sectors, and environmental research [3]. Among metallic nanoparticles, silver nanoparticles (Ag NPs) have received most attention owing to unique conductivity, catalytic, and most important antibacterial, antiviral and antifungal activities [4,5] and have gained popularity in food technology, microbiology, cell biology, chemistry, pharmacology, and parasitology [6]. The protein caps on AgNPs provide significant benefits to attaching bacterial cell surface and stability, which in turn helps human cells bind to and absorb drugs [7].

Synthesis of Ag NPs through physical or chemical methods is more expensive, energy intensive, and requires environmentally unfriendly chemicals [8]. However, green synthesize AgNPs from various plant parts is relatively inexpensive, simple to handle, biocompatible, and ecologically beneficial [9]. Phytochemicals such as enzymes, alkaloids, polysaccharides, tannins, terpenoids, phenols, and vitamins, which are available in all parts of a plant, are responsible for reducing and stabilizing metallic ions in preparing nanoparticles [10,11].

Various studies were reported on Ag NPs synthesis from extracts of various plants such as *Salvia spinosa* [12], *Saccharum officinarum* [13], *Citrus sinensis* [14], *Holoptelea integrifolia* [15], *Ziziphora tenuior* [16], *Berberis brassica nigra, Capsella bursa-pastoris, Lavandula angustifolia* and *Origanum vulgare* [17,18].

Para-nitrophenol, also known as 4-nitrophenol (4-NP), is a phenolic molecule that is utilized as a raw material for preparing insecticides, dyes, pigments, and indicators [19]. The United States Environmental Protection Agency (USEPA) has considered 4-NP a severe environmental pollutant due to its long stability and negative human health effects, which mainly damage the liver, CNS, kidney, etc. even at trace levels [20]. To minimize its environmental effects, various techniques such as chemical precipitation, coagulation, electrocoagulation, biological treatment, catalytic oxidation, adsorption, etc., have been reported [21]. Recently, cost-effective and environmentally friendly methods of reducing 4-NP into less toxic compounds like 4-aminophenol (4-AP) using nanoparticles prepared from extracts of tulsi leaves, *Poria cocos* [1], *Dolichos lablab* [7], *Diospyros malabarica* [23], and *Stachys lavandulifolia* [24] have been reported. The nanoparticles synthesized from plant extracts have high antimicrobial properties against various human pathogens and health treatments.

* Corresponding author.
E-mail address: menge.mtrinity@gmail.com (M. Mulu).

https://doi.org/10.1016/j.btre.2024.e00838
Received 18 January 2024; Received in revised form 15 March 2024; Accepted 20 March 2024
Available online 21 March 2024

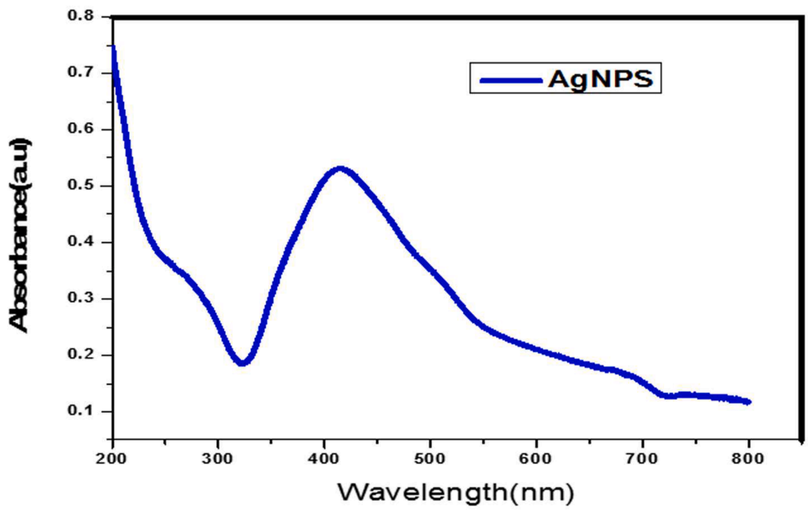

Fig. 1. UV–vis spectra of Ag NPs.

Thus, in this study, the leaf of *Vigna unguiculatus* (cowpea) has been used to synthesize Ag NPs. *V. unguiculata* (L) Walp is a popular legume food crop cultivated in the tropics and subtropics and is consumed by both humans and animals. It is a great source of protein, carbohydrates, and minerals like calcium, iron, zinc, and vitamin A. Vigna unguiculate also contains significant amounts of phytochemical substances like saponins, flavonoids, and phenols. Owing to this, Vigna unguiculate exhibits great potential as a diet for humans and animals and exhibits strong antibacterial and antioxidant activities [25–28].

The Ag NPs were characterized using UV–vis, Fourier-transform infrared (FTIR) spectroscopy, scanning electron microscopy (SEM), transmission electron microscopy (TEM), and X-ray diffraction (XRD). Subsequently, the activities of Ag NPs were evaluated on the reduction of 4-NP and its antibacterial activity against Gram-positive and Gram-negative bacteria.

2. Materials and methods

2.1. Reagents

All chemicals were analytical grades. Ammonia solution (28–30 %), NaOH pellet, H_2SO_4 (98 %), 4-nitrophenol, $NaBH_4$) and $AgNO_3$ were purchased from Sigma-Aldrich (India), while acetone and ethanol were supplied by Himedia (India).

2.2. Preparation of Vigna unguiculata leaf extract

The leaves were washed with Milli-Q water and allowed to dry for 15 days to remove dust particles. Finally, the dried leaves were ground using a grinder (Gx8 Bajaj, India), sieved with a 2 mm mesh, and placed at 4–10 °C in an airtight polyethylene plastic. 2 g of powdered leaves were added to 100 mL of Milli-Q water and heated for 30 min at 80 °C. After cooling down, the mixture was filtered with Whatman No. 42 filter paper, and it was kept in refrigerator, 4 °C for later use.

2.3. Synthesis of Ag NPs

A 1:1 (v,v) extract of *V. unguiculata* (L) Walp and 2 mM $AgNO_3$ solutions were mixed in a 250 mL round-bottomed flask, and sonicated for 15 min to achieve a homogeneous mixture. To this solution, 10 mL NH_3 was added, and refluxed for 1 h via magnetic stirring until an amber-colored solution was formed, indicating Ag NPs synthesis. The stirred mixture was extracted by centrifugation at 15,000 rpm for 15 min, and the precipitate (AgNPs) was washed twice with Milli-Q water followed by ethanol to remove any unreacted plant components.

Plant extract volume, $AgNO_3$ concentration, plant extract concentration, temperature, concentration of NaOH, and time were among the experimental parameters optimized to maximize Ag NPS stability and size.

2.4. Characterization of Ag NPs

The progress of the reaction was evaluated by observing the colour change, and the characteristic aborbation wavelength was assessed through a UV–vis spectrophotometer (Perkin–Elmer Lambda 35 model). The functional groups linked to the Ag NPs were studied with FT-IR (Perkin–Elmer RX-I FT-IR spectrophotometer). The surface morphology and size of AgNPs were examined using SEM (HITACHI S-3000H) and HRTEM. Furthermore, the compositional study was evaluated with energy-dispersive X-ray imaging (EDAX) and X-ray photoelectron spectroscopy (XPS).

2.5. Applications of Ag NPs

2.5.1. Antibacterial activity of Ag NPs

For antibacterial acitivity, Gram-positive bacteria (*B. subtilis* and *Staphylococcus aureus*) and Gram-negative bacteria (Klebsiella pneumonia and *Escherichia coli, E. coli*) was evaluated using the disc diffusion method [29]. In brief, the medium was sterilized with an autoclave at 120 °C for 30 min. Each sterile petri dish was seeded with bacteria strains of interest and transferred aseptically into a 20-mL volume of nutrient agar medium. During the solidification process, the plates were held atroom temperature. A sterile borer was used to drill a single 6 mm-diameter well into each plate. Concentrations ranged between 1 and 5 μg/mL were calculated after the research compounds were reconstituted with appropriate solvents (distilled water). In a 6 mm diameter well, samples, strength, and standard (ciprofloxacin) were all added. The petri plates were held at 37.2 °C for 12 h. Ciprofloxacin (5 g/mL) was used as a standard. The antibacterial activities were estimate by measuring the diameter of inhibition zone.

2.5.2. Catalytic activity of AgNPs

To study the catalytic activity of AgNPs towards reduction of 4-NP, it was carried out by mixing 100 mM NaBH4 with water in a 1:1 molar ratio. To this solution, 100 mL of 1 mM AgNPs were added, and the catalytic acitivity of AgNPS was measured with a UV–vis spectrophotometer.

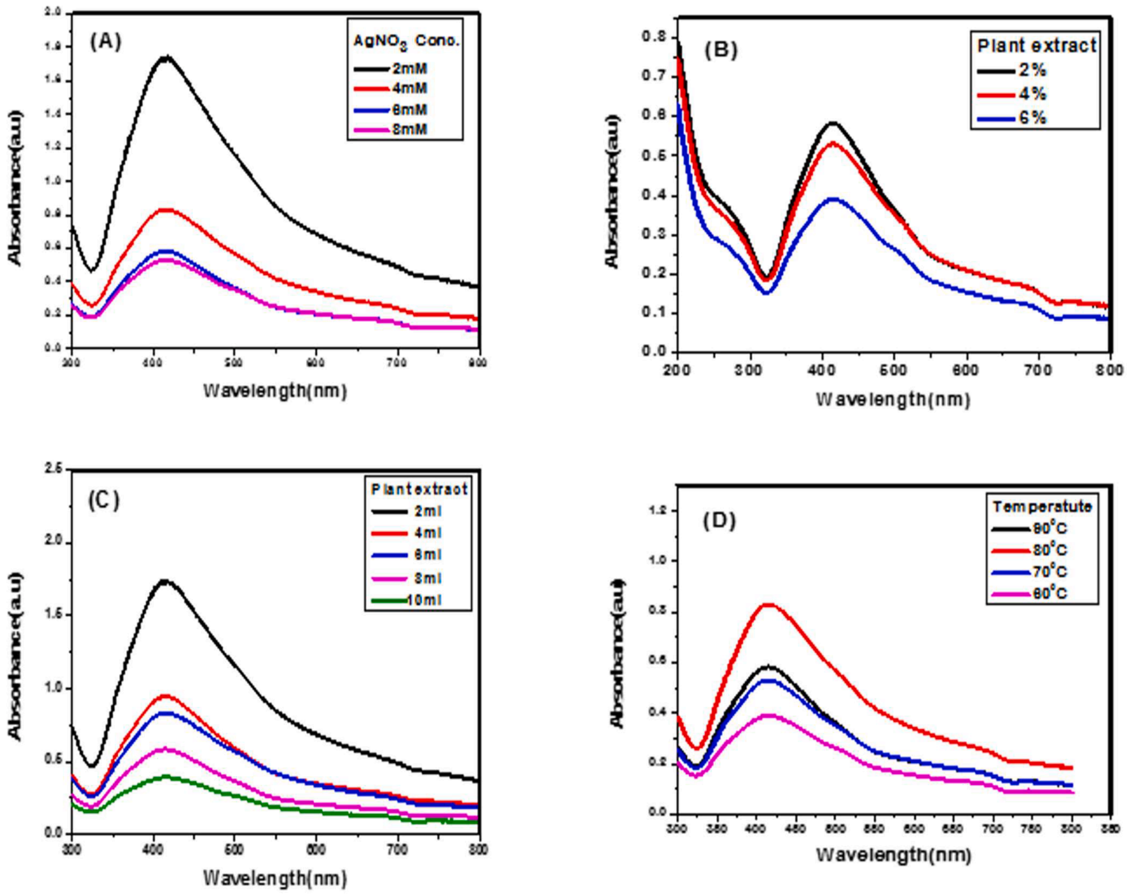

Fig. 2. UV–vis spectra of Ag NPs at (a) different concentrations of $AgNO_3$, (b) different percentage of leaf extracts of *Vigna Unguiculata* (L) Walp plant, (c) different volumes of 2 % of leaf extract of *Vigna Unguiculata* (L) Walp and (d) different temperatures.

3. Results and discussion

3.1. UV–Vs spectroscopy

The color change from yellowish to reddish-brown, then to dark colloidal brown, after the leaf extracts were added to the solution containing aqueous silver nitrate, indicates Ag^+ ions reduction into Ag^o using phytoconstituents extract in the leaf of *V. unguiculata* as a reducing agent according Eqs. (1)–(3) [30].

$$AgNO_3 \leftrightarrow Ag^+(aq) + NO_3{}^-(aq) \quad (1)$$

$$\text{Reducingagent, plant(RA)} \rightarrow RA^+ + e^- \quad (2)$$

$$Ag^+(aq) + e^- \rightarrow Ag^o \quad (3)$$

The change of Ag^+ to Ag^o was further confirmed via the UV–Vis spectrum that appeared around 414 nm (Fig. 1), which showed the creation of surface plasmon resonance (SPR) electrons in AgNPs [31]. As shown in Fig. 2, the stability of AgNPs was studied at various $AgNO_3$ concentrations (2–8 mM), volumes of leaf extracts (2–10 mL), percent of leaf extract (2–6 %) and temperatures (60–90 °C) which affected AgNPs synthesis. The Ag^+ reduction and the amount of AgNPs were maximum when the concentration of $AgNO_3$ was 2 mM, 2 % of plant extract, 2 mL of plant volume, and at a temperature of 80 °C.

3.2. FE-SEM and HR-TEM analysis

The morphology and size of Ag NPs were evaluated using the FE-SEM. As shown in Fig. 3(A–D), the majority of the FE-SEM study shows spherical-shaped Ag NPs with sizes ranged of 9.08–13.06 nm and an average particle size of 11.06 nm. However, high surface energy and high surface area of the produced particles may be responsible for the Ag NPs' agglomeration [32]. The elemental compositions of Ag NPS were determined using EDX. The most intense signal, with a notable quality of around 3.0 keV and a total particle mass of 80 %, indicates the presence of the element silver (Ag^0). Thus it demonstrated the *V. unguiculata* extract mediated bioreduction of Ag^+ ions to elemental silver [33]. Other elements like oxygen and chlorine were also detected in the spectrum with mass percentages of 16.86 % and 3.04 %, respectively, which were associated with the presence of biomolecules in the plant extract [23].

The TEM images (Fig. 4A–C) showed that Ag NPs were well isolated, and most of them are spherical. Fig. 4D, shows the histogram size distribution of AgNPs, with sizes ranging from 1.5 to 21 nm with an average around 11.0 nm, which is in good agreement with the SEM images. The crystalline nature of Ag NPs was also evaluated using selected area electron diffraction (SAED) images and the result showed a diffracted ring pattern, confirming the polycrystalline nature of synthesized Ag NPs (Fig. 4c). This result is in good agreement with the results reported by Kharat & Mendhulkar [34].

3.3. X-ray diffraction (XRD)

XRD is an analytical technique which used for molecular and crystal structures analysis, identification of compounds, quantitative resolving chemical species and to estimate degree of crystallinity. The crystallite sizes (D) of Ag NPs were calculated using Debye–Scherrer according Eq. (4) [35].

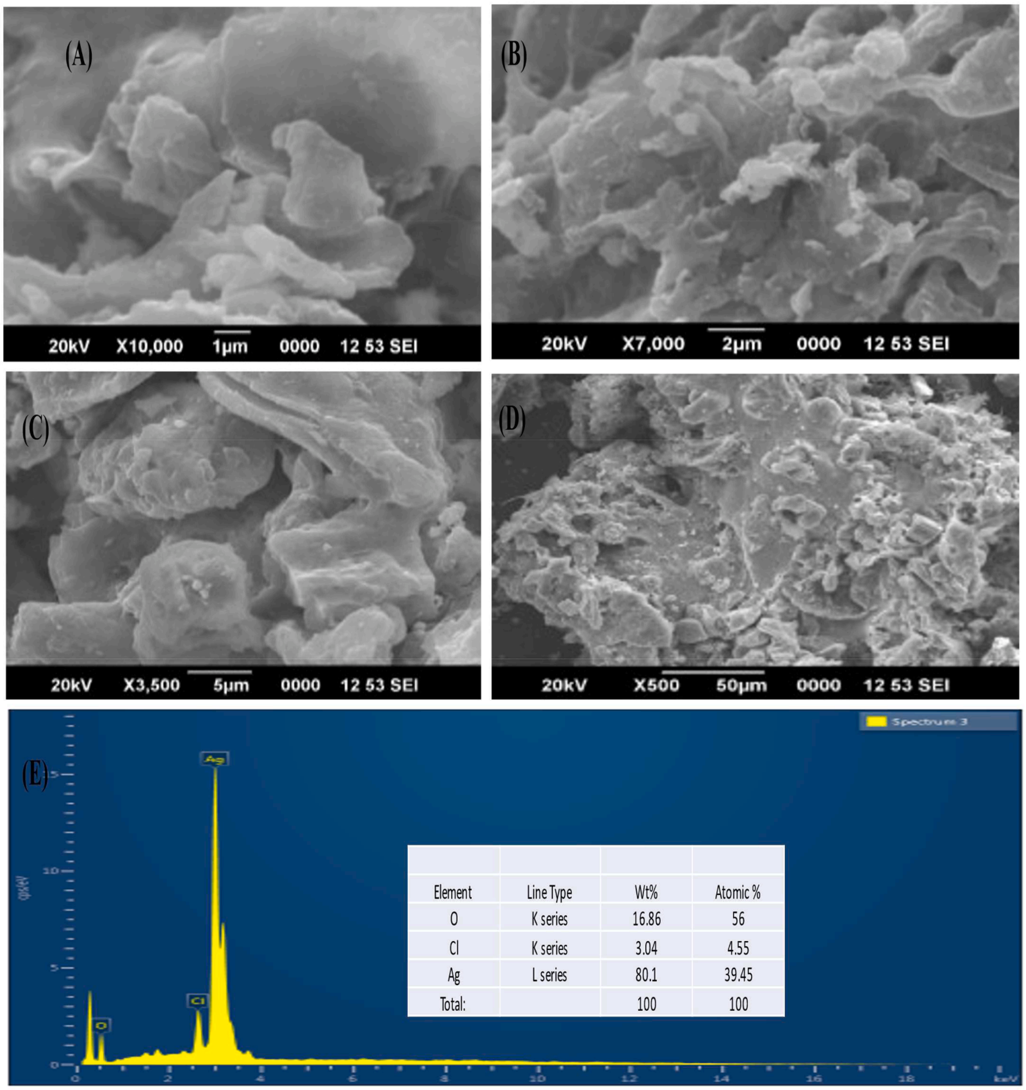

Fig. 3. (a–d) FE-SEM images of *Vigna Unguiculata* (L) Walp plant mediated Ag NPs at different magnifications and (e) EDX spectrum of *Vigna Unguiculata* (L) Walp plant mediated Ag NPS.

$$D = \frac{\lambda k}{\beta \cos\theta} \quad (4)$$

where k is a constant (0.94 for spherical particles), λ is the wavelength of the X-ray radiation (CuKα = 0.1541 nm), β is the full width at half maximum (FWHM) peaks and θ is the Bragg's or difraction angle.

The XRD patterns of Ag NPs (Fig. 5) showed four main diffraction peaks observed at 2θ values of 37.72, 43.87, 64.11 and 77.20, which crosspond to indexed planes the (111), (200), (220), and (311), respectively.

The XRD data indicated the spherical shape of Ag NPs crystalline structure with face centred cubic (fcc) crystalline structure, which is consistant with the TEM analysis. The sizes of the crystals of Ag NPs at (111), (200), (220), and (311) were 11.27, 13.91, 13.75 and 22.68 nm, respectively, with a mean of 14.08 nm (Table 1). These results are consistent with the structure of Ag NPs described in the literature [7,36]. The presence of organic compounds in the leaves and extracts of *V. unguiculata* walp plant leaves that crystallize on the silver surface could be the cause of the unassigned peaks observed at 2θ of 31.86 [37].

3.4. XPS analysis

The physical and chemical states of the synthesized nanoparticles, as well as the actual composition of the materials, are all disclosed by XPS. The XPS data (Fig. 5A–C) at C1S, Ag3d and O1s core levels, which are the indicative for the analysis, strong signals appeared around 368 and 374 eV, with splitting of 6 eV indicating the presence of $3d_{5/2}$ and $3d_{3/2}$ of metallic Ag, respectively [38,39]. The C1s peak detected at 285 eV of binding energy is used as a reference to adjust the binding energy shift, and it also corresponds to sp^2 (C═C) and C–C of the biomolecules in the extract capped with Ag NPs [40]. The spectrum appeared around 531 eV binding energy corresponds to O1s, which attributed to the presence of oxygen atoms in the carboxyl group (–C═O–) bound to the surface of Ag NPs [41].

3.5. Antibacterial activity

The disk diffusion method was used to measure the antibacterial activity of the synthesized Ag NPs against Gram-positive bacteria (*Bacillus subtilis* and *S. aureus*), and Gram-negative bacteria (*E. coli* and *Klebsiella pneumoniae*). The inhibition zone is depicted in Fig. 7 and is represented in Table 1. The plant extract showed a small inhibition zone around the disc in both cases, while the control showed no inhibition zone at all. A comparatively broad inhibition zone against B. cereus growth was observed in the 2-mL extract sample, which may be due to decreased particle size and homogeneous shape as evidenced by SEM

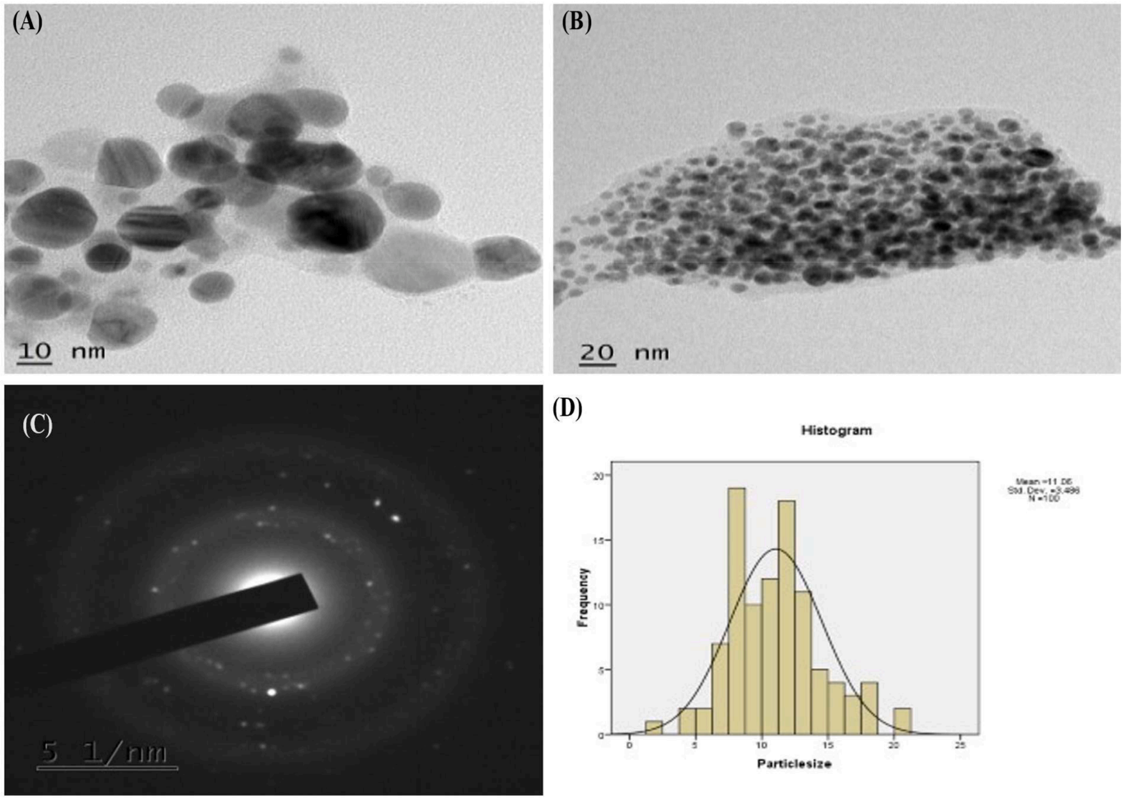

Fig. 4. TEM images of Vigna Unguiculata (L) Walp plant mediated Ag NPs (A) 10 nm scale, (B) 20 nm scale, (C) SAED patterns of Ag NPs, and (D) size distribution histogram of Ag NPs.

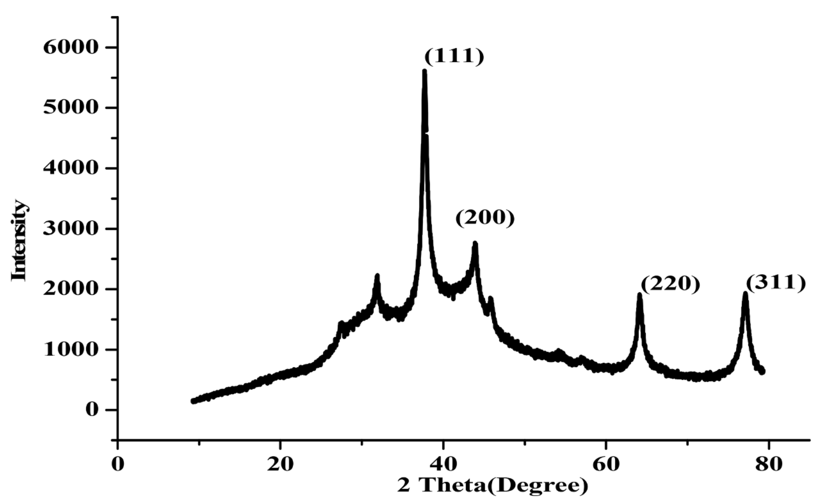

Fig. 5. XRD spectrum of purified Ag-NPs.

Table 1
The estimated crystallite size of Ag NPS.

2Theta (°)	FWHM	*d* value	Crystal size(nm)
31.86491	0.9821815	2.806153	8.79
37.71645	0.7782117	2.383151	11.27
43.87449	0.6433102	2.061881	13.91
64.11035	0.7125706	1.451382	13.75
77.09737	0.4679928	1.236081	22.68
Average			14.08

and TEM tests. Since the small particles have a higher surface-to-volume ratio, they can make more contact with bacteria and easily penetrate the cell wall membrane, causing serious damage. The presence of active silver ions, which are positively charged and attract negatively charged bacteria, is almost definitely responsible for the presence of a large number of silver atoms on the surface of small and spherical-shaped nanoparticles. Silver ions destroyed the bacteria's cell walls and changed the contents of the cell wall [31]. Furthermore, the formation of superoxide anions (O_2), hydroxyl radicals (OH), and hydroxyl radicals inhibits the growth of bacteria, as demonstrated in this study. The Ag NPs showed strong antibacterial activity against Gram-negative bacteria *Escherichia coli* (E. coli) and Klebsiela pneumoniae, as well as

Table 2
The activity diameter of the zone of inhibition (mm) for 50 μL Ag NPS and constant diameter of the well = 6 mm.

Organisms	1	2	3	4 (Control/ H_2O)	5	6 (standard/ Ciprofloxacin)	7
Bacillus pumilus	23	22	15	–	14	40	10
Staphylococcus aureus	29	25	20	–	15	40	8
Escherichia coli	15	13	12	–	10	40	–
Klebsiella pneumoniae	17	19	16	–	16	40	15

*Numbers along the organisms' row stands for concentration of Ag NPs (1, 2, 3, 5 & 7): 4 and 6 represents water and standard, respectively.

Gram-positive bacteria *B. pumilus* and S. aeurus bacteria. The average zone of inhibition for the bacteria Staphylococcus aeurus, Bacillus pumilusn Klebsiela pneumonia and *E. coli* were 29 mm, 23 mm, 17 mm and 15 mm, respectively. In this study, the zone of inhibition of Ag NPS was compared to that of a reference antibiotic drug (Ciprofloxacin). The Ag NPS have an overall inhibition zone of 29 mm against *S. aureus* and a minimum inhibition zone of 10 mm against *E. coli* bacteria (Table 2). The minimum inhibitory concentration (MIC) in μg/mL of the AgNPS for the tested Gram-positive bacteria (*B. subtilis*,and *S. aureus*), Gram-negative bacteria (*E. coli*, and *K. pneumoniae*) were summarized in Table 2. The MIC values which provided the highest zone of inhibition for *B. pumilus, S. aureus*, and *E. coli* were 1 μg/mL, while for Klebsiella pneumonia were 2 μg/mL (Fig. 6).

The antibacterial activity of Ag NPS against bacteria (*B. subtilis*), *S. aureus, Escherichia coli* (E. coli), and *K. pneumoniae* (KP) was also reported at higher concentrations. The antimicrobial potency obtained in this study was in the order of *S. aureus* > *B. pumilus* > Klebsiella pneumonia > *E. coli*. The antibacterial activities towards various bacteria were due to synergistic effect between Ag NPs and the plant extract [42].

The zones of inhibition of AgNPS against several bacteria were also compared with literature reports. As can be seen in Table 3, the ZOI for E. coli is comparable with AgNPS synthesized with *Ficus hispida* Linn [43], fenugreek [44], tea [45], *Lysiloma acapulcensis* [46]. However, the ZOI of AgNPS against E. coli was found to be higher than that of *Talinum triangulare* [47], *Dolichos lablab* [7], *D. malabarica* [23], and *Saussurea obvallata* [48]. The ZOI of AgNPS against *S. aureus* was also significantly higher than the reported values [23,44,46–50]. Finally, the ZOI of AgNPS synthesized from *V. unguiculata* against Klebsiella pneumonia was higher than the ZOI of tea[45].

3.6. Reduction of 4-nitrophenol

It is established that metal nanoparticles have strong catalytic activity in hydrogenation, and reduction of various pollutants such as nitrophenol, dyes, etc.[50]. The catalytic activity of Ag NPs was evaluated by reducing 4-NP in sodium borohydride. The UV–Vis spectrum of 4-NP showed an absorpation peak around 318 nm, while in the presence of reductant ($NaBH_4$) a new peak was appeared around 401 nm due to formation of the 4-nitrophenolate ion in alkaline media which is bright yellow in color (Fig. 8). In the presence of Ag NPs as catalyst, the color of 4-NP become faded completely and declined absorption intensity due to the formation of 4-aminophenol, which signifies the efficient catalytic potential of synthesized Ag NPs. This due to the fact that AgNPs enhancing the reactant adsorption on their surface and lowering the kinetic energy barrier, thus AgNPs speed up the rate of reaction [22]. The characteristic reduction peak of 4-NP at 401 nm decreased in intensity as the reaction progressed, while the characteristic peak of development of 4-AP at 300 nm increased as a result of the production of 4-aminophenol (Fig. 9).

4. Conclusion

Proteins and flavonoids in the *V. Unguiculata* leaf extract are essential in the formation of silver nanoparticles in this sample. A green synthesis

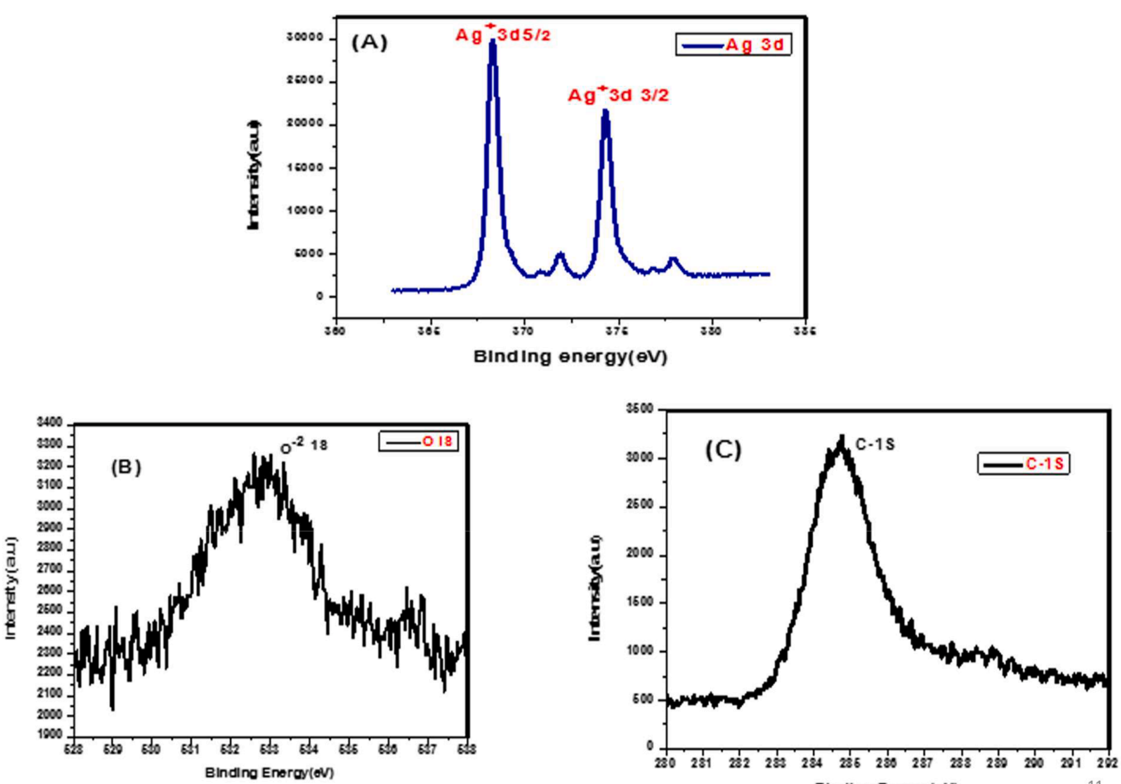

Fig. 6. XPS spectra of the green synthesized silver nanoparticles of (A) Ag 3d, (B) O 1 s and (c) C 1 s.

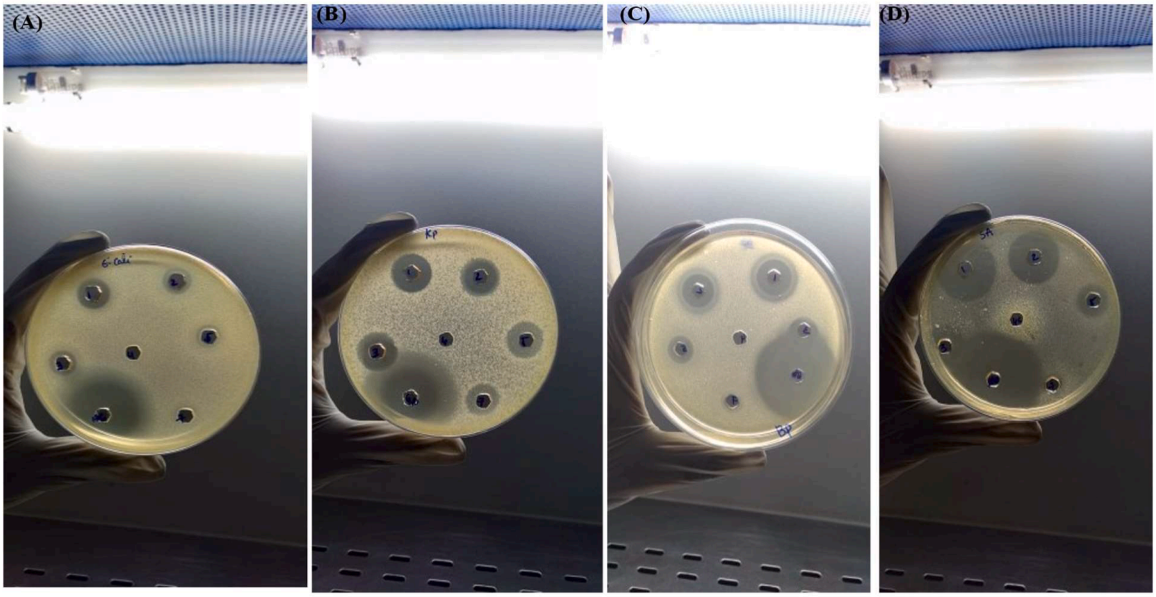

Fig. 7. Antimicrobial activity of Ag NPS against Escherichia coli (E. coli) (B)*Klebsiella pneumoniae* (KP) (C) *Bacillus pumilus* (BP) (D) *Staphylococcus aureus* (SA)(S-standard (Ciprofloxacin), C- Control (water).

Table 3
Comparison of the zone of inhibition of AgNPs in this study with literature reports.

Plant	Ag NPS size (nM)	zone of inhibition (mm)				Refe.
		E. coli	*S. aureus*	*K. pneumoniae*	*B. pumilus*	
Dolichos lablab	9	12.02	–	–	–	[7]
Diospyros malabarica	17.4	8.4–12.1	6.1–13.1	–	–	[23]
Ficus hispida Linn	20	14	–	–	–	[43]
Fenugreek	20–30	16.27	12.47	–	–	[44]
Tea	4.06	15	–	10	–	[45]
Lysiloma acapulcensis	1.2–62	18	16	–	–	[46]
Talinum triangulare	–	2.55	2.35	–	–	[47]
Saussurea obvallata	12	10–12	10–13	–	–	[48]
Alstonia scholaris	50	–	1–2.5	–	–	[49]
Vigna unguiculata	11.08	15	29	17	23	This study

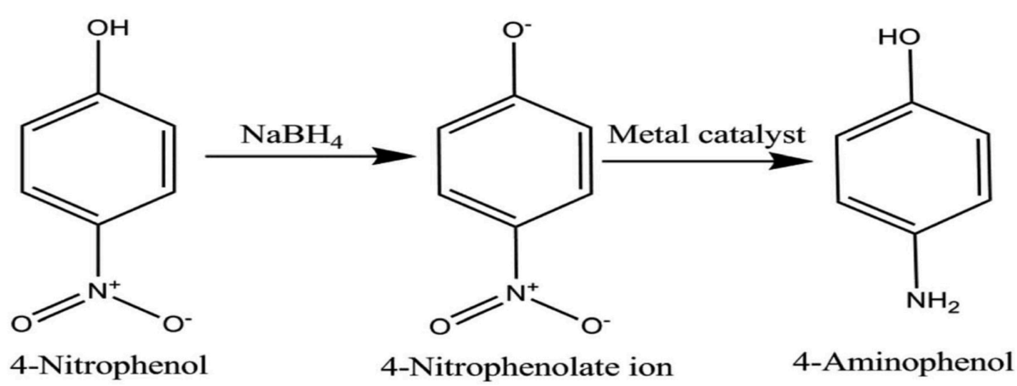

Fig. 8. The mechanism of 4-nitrophenol reduction.

process using *V. Unguiculata* leaf extract as the reducing agent was effective in producing spherical-shaped Ag NPs. The blue-shifting in the SPR peaks indicates the size reduction of Ag NPs with leaf extract concentrations. The face-centered cubic structure of the synthesized Ag NPs was confirmed by XRD studies in all cases, with crystallites preferentially aligned along the (111) plane of the silver crystals. For the 2-mL extract-prepared Ag NPs, the measured crystallite size decreased dramatically from 20 to 10 nm. The, SEM spectrum showed that shaped Ag NPs was spherical. The presence of silver, as well as other elements (Cl and O) in the plant, was confirmed by the EDAX spectrum. Biologically synthesized Ag NPs had better antibacterial activity against Gram-positive bacteria (*B. subtilis*), *S. aureus*, and Gram-negative bacteria *Escherichia coli* (E. coli) and *K. pneumoniae* (KP), suggesting that they could be used in a variety of biomedical applications. In the presence of bacteria *S. aureus* and *B. pumilus*, Ag interstitial and Ag vacancies with smaller spherical Ag NPs increased electron density, resulting in MICs of

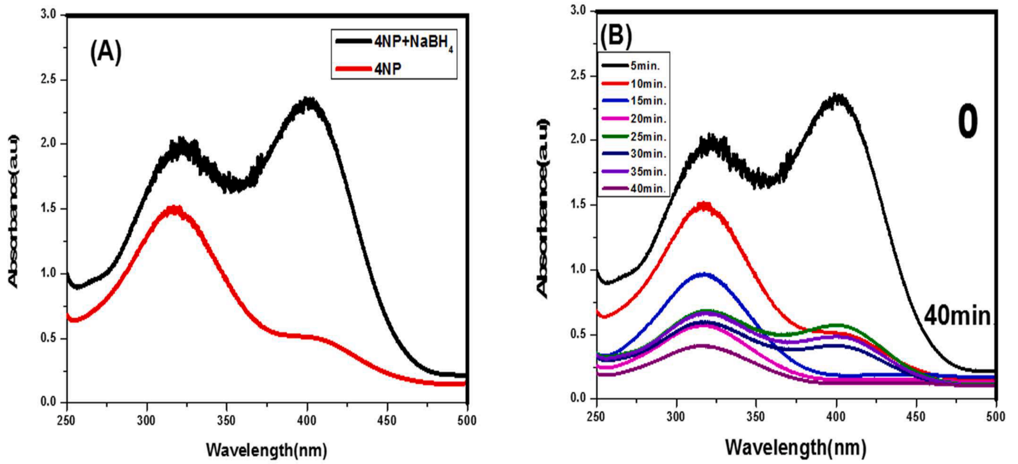

Fig. 9. UV–vis spectra of (A) 4-NP alone and formation of 4-Nitrophenolate ion in the presence of $NaBH_4$ and (B) reduction of 4-NP to 4-AP in presence of $NaBH_4$ and Ag NPs with time.

72.5 % and 57.5 %, respectively. As a result, these biologically prepared Ag NPs can be used to kill microorganisms that can be found everywhere and affect our food, as well as other agricultural products derived from industrial effluents.

The results of antibacterial sensitivity confirmed the Ag NPS has antibacterial activity which showed maximum zone of inhibition against the *B. pumilus* (29 mm) and minimum against *E. coli* (15 mm) bacteria. Furthermore, the activity result confirmed the bactericidal activity of Ag NPS against Gram-positive bacteria (*B. subtilis*), *S. aureus*, and Gram-negative bacteria *E. coli* (E. coli) and *K. pneumoniae* (KP) bacteria and Ag NPS behaves as bactericidal at higher concentration.

Ethics approval

All experimental procedures did not include any animal or human element

CRediT authorship contribution statement

Mengistu Mulu: Writing – original draft, Methodology, Investigation, Conceptualization. **Molla Tefera:** Writing – review & editing, Visualization, Methodology, Funding acquisition, Data curation. **Atnafu Guadie:** Writing – review & editing, Validation, Methodology, Data curation, Conceptualization. **K. Basavaiah:** Writing – review & editing, Validation, Supervision, Data curation.

Declaration of competing interest

The authors declare that they have no known competing financial interests or personal relationships that could have appeared to influence the work reported in this paper.

Data availability

The data that has been used will be available on request.

References

[1] V.D. Doan, T.L. Phan, Y. Vasseghian, L.O. Evgenievna, Efficient and fast degradation of 4-nitrophenol and detection of Fe (III) ions by Poria cocos extract stabilized silver nanoparticles, Chemosphere 286 (2022) 131894.
[2] C. Karaman, O. Karaman, N. Atar, L.M. Yola, Electrochemical immunosensor development based on core-shell high-crystalline graphitic carbon nitride@carbon dots and Cd0.5Zn0.5S/d-Ti3C2Tx MXene composite for heart-type fatty acid–binding protein detection, Microchim. Acta 188 (2021) 182.
[3] S. Akgöl, F. Ulucan-Karnak, C.I. Kuru, K. Kuşat, The usage of composite nanomaterials in biomedical engineering applications, Biotechnol. Bioeng. 118 (8) (2021) 2906–2922.
[4] S. Ahmed, M. Ahmad, B.L. Swami, S. Ikram, A review on plants extract mediated synthesis of silver nanoparticles for antimicrobial applications: a green expertise, J. Adv. Res. 7 (1) (2016) 17–28.
[5] N.S. Alharbi, N.S. Alsubhi, A.I. Felimban, Green synthesis of silver nanoparticles using medicinal plants: characterization and application, J. Radiat. Res. Appl. Sci. 15 (3) (2022) 109–124.
[6] C. Vanlalveni, S. Lallianrawna, A. Biswas, M. Selvaraj, B. Changmai, S.L. Rokhum, Green synthesis of silver nanoparticles using plant extracts and their antimicrobial activities: a review of recent literature, RSC Adv. 11 (5) (2021) 2804–2837.
[7] M.H. Kahsay, D. RamaDevi, Y.P. Kumar, B.S. Mohan, A. Tadesse, G. Battu, K. Basavaiah, Synthesis of silver nanoparticles using aqueous extract of Dolichos lablab for reduction of 4-Nitrophenol, antimicrobial and anticancer activities, OpenNano 3 (2018) 28–37.
[8] K. Zawadzka, A. Felczak, M. Nowak, A. Kowalczyk, I. Piwoński, K. Lisowska, Antimicrobial activity and toxicological risk assessment of silver nanoparticles synthesized using an eco-friendly method with Gloeophyllum striatum, J. Hazard. Mater. 418 (2021) 126316.
[9] R. Arif, R. Uddin, A review on recent developments in the biosynthesis of silver nanoparticles and its biomedical applications, Med. Devices Sens. 4 (1) (2021) e10158.
[10] M. Aslam, A.Z. Abdullah, M. Rafatullah, Recent development in the green synthesis of titanium dioxide nanoparticles using plant-based biomolecules for environmental and antimicrobial applications, J. Ind. Eng. Chem. 98 (2021) 1–16.
[11] S. Jadoun, R. Arif, N.K. Jangid, R.K. Meena, Green synthesis of nanoparticles using plant extracts: a review, Environ. Chem. Lett. 19 (1) (2021) 355–374.
[12] S. Pirtarighat, M. Ghannadnia, S. Baghshahi, Green synthesis of silver nanoparticles using the plant extract of Salvia spinosa grown in vitro and their antibacterial activity assessment, J. Nanostructure Chem. 9 (2019) 1–9.
[13] S. Jadoun, R. Arif, N.K. Jangid, R.K. Meena, Green synthesis of nanoparticles using plant extracts: a review, Environ. Chem. Lett. 19 (2021) 355–374.
[14] K.N. Nahar, M. Rahaman, G. Khan, M. Islam, S.M. Al-Reza, Green synthesis of silver nanoparticles from Citrus sinensis peel extract and its antibacterial potential, Asian J. Green Chem. 5 (2021) 135–150.
[15] V. Kumar, S. Singh, B. Srivastava, R. Bhadouria, R. Singh, Green synthesis of silver nanoparticles using leaf extract of Holoptelea integrifolia and preliminary investigation of its antioxidant, anti-inflammatory, antidiabetic and antibacterial activities, J. Environ. Chem. Eng. 7 (3) (2019) 103094.
[16] B. Sadeghi, F. Gholamhoseinpoor, A study on the stability and green synthesis of silver nanoparticles using Ziziphora tenuior (Zt) extract at room temperature, Spectrochim. Acta Part A: Mol. Biomol. Spectrosc. 134 (2015) 310–315.
[17] M.R. Shaik, M. Khan, M. Kuniyil, A. Al-Warthan, H.Z. Alkhathlan, M.R.H. Siddiqui, J.P. Shaik, A. Ahamed, A. Mahmood, M. Khan, et al., Plant-extract-assisted green synthesis of silver nanoparticles using Origanum vulgare L. extract and their microbicidal activities, Sustainability 10 (2018) 913.
[18] A. Salayová, Z. Bedlovičová, N. Daneu, M. Baláž, Z. Lukáčová Bujňáková, Ľ. Balážová, Ľ. Tkáčiková, Green synthesis of silver nanoparticles with antibacterial activity using various medicinal plant extracts: morphology and antibacterial efficacy, Nanomaterials 11 (4) (2021) 1005.
[19] H. Yu, S. Oh, Y. Han, S. Lee, H.S. Jeong, H.J. Hong, Modified cellulose nanofibril aerogel: tunable catalyst support for treatment of 4-Nitrophenol from wastewater, Chemosphere 285 (2021) 131448.
[20] M. Zarei, J. Bahrami, M. Zarei, Zirconia nanoparticle-modified graphitic carbon nitride nanosheets for effective photocatalytic degradation of 4-nitrophenol in water, Appl. Water Sci. 9 (2019) 1–11.
[21] M. Ramalingam, V.K. Ponnusamy, S.N. Sangilimuthu, Electrochemical determination of 4-nitrophenol in environmental water samples using porous

graphitic carbon nitride-coated screen-printed electrode, Environ. Sci. Pollut. Res. 27 (2020) 17481–17491.
[22] M.A. Adebayo, F.I. Areo, Removal of phenol and 4-nitrophenol from wastewater using a composite prepared from clay and Cocos nucifera shell: kinetic, equilibrium and thermodynamic studies, Resour., Environ. Sustain. 3 (2021) 100020.
[23] J. Singh, A. Mehta, M. Rawat, S. Basu, Green synthesis of silver nanoparticles using sun dried tulsi leaves and its catalytic application for 4-Nitrophenol reduction, J. Environ. Chem. Eng. 6 (1) (2018) 1468–1474.
[24] K.K. Bharadwaj, B. Rabha, S. Pati, B.K. Choudhury, T. Sarkar, S.K. Gogoi, H. A. Edinur, Green synthesis of silver nanoparticles using Diospyros malabarica fruit extract and assessments of their antimicrobial, anticancer and catalytic reduction of 4-nitrophenol (4-NP), Nanomaterials 11 (8) (2021) 1999.
[25] M. Shahriary, H. Veisi, M. Hekmati, S. Hemmati, In situ green synthesis of Ag nanoparticles on herbal tea extract (Stachys lavandulifolia)-modified magnetic iron oxide nanoparticles as antibacterial agent and their 4-nitrophenol catalytic reduction activity, Mater. Sci. Eng.: C 90 (2018) 57–66.
[26] M.S. Alidu, I.K. Asante, H.K. Mensah, Evaluation of nutritional and phytochemical variability of cowpea Recombinant Inbred Lines under contrasting soil moisture conditions in the Guinea and Sudan Savanna Agro-ecologies, Heliyon 6 (2) (2020).
[27] J.M. Dinore, H.S. Patil, B.S. Dobhal, M. Farooqui, Phytochemical analysis by GC-MS, LC-MS complementary approaches and antimicrobial activity investigation of Vigna unguiculata (L.) Walp. leaves, Nat. Prod. Res. 36 (21) (2022) 5631–5637.
[28] P.A.E.D. Sombié, M. Compaoré, A.Y. Coulibaly, J.T. Ouédraogo, J.B.D.L. S. Tignégré, M. Kiendrébéogo, Antioxidant and phytochemical studies of 31 cowpeas (Vigna unguiculata (L. Walp.)) genotypes from Burkina Faso, Foods 7 (9) (2018) 143.
[29] M.T. Tzanova, T.D. Stoilova, M.H. Todorova, N.Y. Memdueva, M.A. Gerdzhikova, N.H. Grozeva, Antioxidant potentials of different genotypes of cowpea (Vigna unguiculata L. Walp.) cultivated in Bulgaria, Southern Europe, Agronomy 13 (7) (2023) 1684.
[30] A. Kaur, S. Preet, V. Kumar, R. Kumar, R. Kumar, Synergetic effect of vancomycin loaded silver nanoparticles for enhanced antibacterial activity, Colloids Surf. B: Biointerfaces 176 (2019) 62–69.
[31] M. Rafique, I. Sadaf, M.B. Tahir, M.S. Rafique, G. Nabi, T. Iqbal, K. Sughra, Novel and facile synthesis of silver nanoparticles using Albizia procera leaf extract for dye degradation and antibacterial applications, Mater. Sci. Eng.: C 99 (2019) 1313–1324.
[32] Hemlata, P.R. Meena, A.P. Singh, K.K. Tejavath, Biosynthesis of silver nanoparticles using Cucumis prophetarum aqueous leaf extract and their antibacterial and antiproliferative activity against cancer cell lines, ACS Omega 5 (10) (2020) 5520–5528.
[33] P. Anbu, S.C. Gopinath, M.N. Salimi, I. Letchumanan, S. Subramaniam, Green synthesized strontium oxide nanoparticles by Elodea canadensis extract and their antibacterial activity, J. Nanostructure Chem. (2022) 1–9.
[34] K.F. Princy, A. Gopinath, Green synthesis of silver nanoparticles using polar seaweed Fucus gardeneri and its catalytic efficacy in the reduction of nitrophenol, Polar Sci. 30 (2021) 100692.
[35] S.N. Kharat, V.D. Mendhulkar, Synthesis, characterization and studies on antioxidant activity of silver nanoparticles using Elephantopus scaber leaf extract, Mater. Sci. Eng.: C 62 (2016) 719–724.
[36] M.B. Mobarak, M.S. Hossain, F. Chowdhury, S. Ahmed, Synthesis and characterization of CuO nanoparticles utilizing waste fish scale and exploitation of XRD peak profile analysis for approximating the structural parameters, Arab. J. Chem. 15 (10) (2022) 104117.
[37] H. Yousaf, A. Mehmood, K.S. Ahmad, M. Raffi, Green synthesis of silver nanoparticles and their applications as an alternative antibacterial and antioxidant agents, Mater. Sci. Eng.: C 112 (2020) 110901.
[38] V. Kathiravan, Green synthesis of silver nanoparticles using different volumes of Trichodesma indicum leaf extract and their antibacterial and photocatalytic activities, Res. Chem. Intermed. 44 (9) (2018) 4999–5012.
[39] F. Gulbagca, S. Ozdemir, M. Gulcan, F. Sen, Synthesis and characterization of Rosa canina-mediated biogenic silver nanoparticles for anti-oxidant, antibacterial, antifungal, and DNA cleavage activities, Heliyon 5 (12) (2019).
[40] G. Liao, J. Chen, W. Zeng, C. Yu, C. Yi, Z. Xu, Facile preparation of uniform nanocomposite spheres with loading silver nanoparticles on polystyrene-methyl acrylic acid spheres for catalytic reduction of 4-nitrophenol, J. Phys. Chem. C 120 (45) (2016) 25935–25944.
[41] N. Jayarambabu, S. Velupla, A. Akshaykranth, N. Anitha, T.V. Rao, Bambusa arundinacea leaves extract-derived Ag NPs: evaluation of the photocatalytic, antioxidant, antibacterial, and anticancer activities, Appl. Phys. A 129 (1) (2023) 13.
[42] P. Attri, S. Garg, J.K. Ratan, A.S. Giri, Silver nanoparticles from Tabernaemontana divaricate leaf extract: mechanism of action and bio-application for photo degradation of 4-aminopyridine, Environ. Sci. Pollut. Res. 30 (10) (2023) 24856–24875.
[43] G. Liao, Y. Gong, C. Yi, Z. Xu, Soluble, antibaterial, and anticorrosion studies of sulfonated polystyrene/polyaniline/silver nanocomposites prepared with the sulfonated polystyrene template, Chin. J. Chem. 35 (7) (2017) 1157–1164.
[44] A. Ramesh, D. Devi, G. Battu, K. Basavaiah, A Facile plant mediated synthesis of silver nanoparticles using an aqueous leaf extract of Ficus hispida Linn. f. for catalytic, antioxidant and antibacterial applications, S. Afr. J. Chem. Eng. 26 (2018) 25–34.
[45] P.V. Sagar, D. Ramadevi, K. Basavaiah, S.M. Botsa, Green synthesis of silver nanoparticles using aqueous leaf extract of Saussurea obvallata for efficient catalytic reduction of nitrophenol, antioxidant, and antibacterial activity, Water Sci. Eng. (2023) 1–11.
[46] O.A. Ojo, B.E. Oyinloye, A.B. Ojo, O.B. Afolabi, O.A. Peters, O. Olaiya, O. Osunlana, Green synthesis of silver nanoparticles (AgNPs) using Talinum triangulare (Jacq.) Willd. leaf extract and monitoring their antimicrobial activity, J. Bionanosci. 11 (4) (2017) 292–296.
[47] B. Senthil, T. Devasena, B. Prakash, A. Rajasekar, Non-cytotoxic effect of green synthesized silver nanoparticles and its antibacterial activity, J. Photochem. Photobiol. B: Biol. 177 (2017) 1–7.
[48] Y.Y. Loo, Y. Rukayadi, M.A.R. Nor-Khaizura, C.H. Kuan, B.W. Chieng, M. Nishibuchi, S. Radu, In vitro antimicrobial activity of green synthesized silver nanoparticles against selected gram-negative foodborne pathogens, Front. Microbiol. 9 (2018) 379304.
[49] D. Garibo, H.A. Borbón-Nuñez, J.N.D. de León, E. García Mendoza, I. Estrada, Y. Toledano-Magaña, A. Susarrey-Arce, Green synthesis of silver nanoparticles using Lysiloma acapulcensis exhibit high-antimicrobial activity, Sci. Rep. 10 (1) (2020) 12805.
[50] P. Shetty, N. Supraja, M. Garud, T.N.V.K.V. Prasad, Synthesis, characterization and antimicrobial activity of Alstonia scholaris bark-extract-mediated silver nanoparticles, J. Nanostructure Chem. 4 (2014) 161–170.